NEWTONIAN DYNAMICS OF TIME-DEPENDENT MEAN FIELD THEORY

A. BONASERA, G.F. BERTSCH and E.N. EL-SAYED
Cyclotron Laboratory, Michigan State University, East Lansing, MI 48824, USA

Received 6 February 1984

Force equations describing heavy ion collisions are derived from the continuum limit of time-dependent mean field theory. The equations mimic the actual behavior of finite nucleus TDHF quite well, and might serve as a starting point for a more complete theory.

In this note we investigate a single model for low energy heavy ion collisions [1], based on the dynamics of time-dependent mean field theory (TDHF). The theory is reduced to the newtonian mechanics of two nuclear centers interacting via classical forces. In view of the many force models that have been put forth already [2–4], it is natural to ask what the point is of yet another such model. Our objective is to understand the fundamental dynamics of the reactions, and this requires a model that is consistent with our present theoretical framework. At present, the TDHF is the best justified theory at a fundamental level, although it is obviously incomplete in several respects and needs to be extended. Because of the computational difficulties of the theory, extensions are unmanageable unless a simple modelling is found for TDHF itself. Our efforts are directed to that end.

The most important dynamic variable in a simplified description is the separation coordinate between the colliding nuclei, r. We begin with a precise definition of that quantity. Consider a plane between the two nuclei chosen so that the expectation of nucleon number on each side remains fixed. Calling the two sies A and B, the separation coordinate may be defined as the integral over the single-particle density,

$$r = \int_{\mathrm{A}} \rho(r')r'\,\mathrm{d}^3r' - \int_{\mathrm{B}} \rho(r')r'\,\mathrm{d}^3r' \,. \tag{1}$$

In a like manner the momentum of one of the nuclei may be defined

$$p_{\mathrm{A}} = \int_{\mathrm{A}} \mathrm{d}^3r((\vec{\nabla} - \vec{\nabla}')/2\mathrm{i})\rho^{(1)}(r, r')|_{r=r'} \,. \tag{2}$$

The dynamic equation is found by taking the time derivative of eq. (2), using the hamiltonian to evaluate the derivative of the wave function. In TDHF the hamiltonian is a single-particle operator and the dynamic equation becomes

$$\frac{\mathrm{d}p_{\mathrm{A}}}{\mathrm{d}t} = \frac{1}{\mathrm{i}} \int_{\mathrm{A}} \sum_i [\phi_i^*((\vec{\nabla} - \overleftarrow{\nabla})/2\mathrm{i})H\phi_i - (H\phi_i^*)((\vec{\nabla} - \overleftarrow{\nabla})/2\mathrm{i})\phi_i]\,\mathrm{d}^3r \,. \tag{3}$$

Here ϕ_i are the single-particle wave functions and H is the TDHF hamiltonian. The terms in eq. (3) involving the kinetic energy operator are simplified in the usual way using integration by parts, leaving a surface integral. We assume that the mean field potential depends only on the single-particle density, permitting an arbitrary functional dependence on that density. The contribution of the short range part of the potential field can then also be expressed as a surface integral on the dividing plane. The resulting equation for the acceleration has the form

$$\frac{\mathrm{d}p_{\mathrm{A}}}{\mathrm{d}t} = \int_{\mathrm{S}} \mathrm{d}^2r[\hat{\boldsymbol{n}}\cdot\boldsymbol{\Pi} + \hat{\boldsymbol{n}}(\rho\,\partial U/\partial\rho - U)] + \int_{\mathrm{A}} \mathrm{d}^3r \int_{\mathrm{B}} \mathrm{d}^3r' \frac{\rho_{\mathrm{p}}(r)\rho_{\mathrm{p}}(r')e^2}{|r-r'|^3}(r-r') \,. \tag{4}$$

0.370-2693/84/$ 03.00

The first term is a surface integral involving the particle momentum flux tensor

$$\Pi_{\alpha\beta} = \frac{1}{m}\sum_i \phi_i^*((\vec{\nabla} - \overleftarrow{\nabla})/2\mathrm{i})_\alpha((\vec{\nabla} - \overleftarrow{\nabla})/2\mathrm{i})_\beta\phi_i\,, \qquad (5)$$

and a potential field contribution, which is expressed in terms of the potential energy density associated with the short-range part of the interaction [5], U. The dividing plane is denoted by S and the normal to this surface by $\hat{\boldsymbol{n}}$. The Coulomb force is given by the second integral in the equation. Eq. (4) is expressed in a form particularly convenient for reduction to classical dynamics. We expect on physical grounds that the force between the two nuclei depends only on the state of the system at the surface of contact, except for the long range Coulomb interaction. Eq. (4) has this form, with the first term in the surface integral arising from the exchange of nucleons between two nuclei. The second term is the force arising from the nuclear potential field. At large separations, the potential dominates because the potential field extends farther than the particle densities. At close contact, the two terms tend to cancel, and the residual force depends sensitively on the momentum distribution of the nucleons and the compressibility modulus associated with the hamiltonian.

In principle, the full TDHF wave function is still needed to calculate the right-hand side of eq. (4); our model is a set of simplifying assumptions about how the TDHF behaves. We shall approximate the TDHF density matrix by its value in bulk nuclear matter, together with a surface correction. Parametrizing the contact surface S as a circle of radius r_n, eq. (4) is reduced to

$$\mathrm{d}p_\mathrm{A}/\mathrm{d}t = \pi r_\mathrm{n}^2\hat{\boldsymbol{n}}\cdot[\boldsymbol{\Pi} + \mathbf{1}(\rho\delta U/\delta\rho - U)]_\mathrm{NM} + 2\pi\sigma r_\mathrm{n}\hat{\boldsymbol{n}} + (Z_1Z_2e^2/r^2)\hat{\boldsymbol{n}}\,. \qquad (6)$$

The bulk contribution is given by the first term on the right, with the subscript NM denoting a nuclear matter approximation. The surface contribution is proportional to σ, which we take to be the empirical surface energy, $\sigma = 0.9\,\mathrm{MeV/fm^2}$. For the calculations below, we treat the Coulomb interaction in the monopole–monopole approximation, which is quite accurate for lighter nuclei.

In mean field theory, the density matrix for two colliding slabls of nuclear matter is described by two intersecting Fermi surfaces which may become distorted from spherical shape by potential field effects. If the compressibility of nuclear matter is that of a free Fermi gas, which seems to be close to the empirical situation, then the surfaces are just the Fermi spheres of the individual slabs. The particle flux tensor was evaluated to lowest order in the relative velocity of the two Fermi spheres, $\boldsymbol{v}_{nm}$ by Randrup [6] to give a momentum flux across the surface

$$\hat{\boldsymbol{n}}_0\,[\boldsymbol{\Pi} + \mathbf{1}(\rho\delta U/\delta\rho - U)]_\mathrm{NM} \cong \tfrac{3}{16}\rho v_\mathrm{F} m(\hat{\boldsymbol{n}}\hat{\boldsymbol{n}}\cdot\boldsymbol{v}_{nm} + \boldsymbol{v}_{nm}). \qquad (7)$$

Here v_F is the Fermi velocity. Randrup further replaced v_{nm} by $\mathrm{d}r/\mathrm{d}t$, in effect assuming that all parts of the nucleus have the same motion. This reduces the force to a linear friction. However, the Fermi surface in mean field dynamics depends on the motion of the boundary of the nucleus at an earlier time, resulting in a lag [7] between the center of mass motion and the local Fermi surface at S. The delay time is certainly more than the nucleon transit time, and is less than twice the transit time. Within these limits, we shall leave the delay time as a parameter, writing it as

$$t_\mathrm{D} = \alpha t_0\,, \quad t_0 = 2R/v_\mathrm{F}\,,$$

where $1 < \alpha < 2$. The transverse part of v_{nm} has contributions both from the center of mass motion and from the internal angular momentum of the individual nuclei. Our model for v_{nm} is then

$$\boldsymbol{v}_{nm}(t) = (\mathrm{d}r/\mathrm{d}t)(t - t_\mathrm{D}) + \hat{\boldsymbol{s}}(R_\mathrm{A}l_\mathrm{A}/I_\mathrm{A} - R_\mathrm{B}l_\mathrm{B}/I_\mathrm{B})\,, \qquad (8)$$

where R, l, and I are the radii, angular momentum, and moment of inertia of the nuclei, and s is a unit vector in the reaction plane. The angular momentum can be found from the integration of the force equation, so the only need for a finite nucleus TDHF calculation is the determination of the evolution of the neck radius.

The dynamics of the neck region are quite different when the two nuclei approach each other than when they rebound. The TDHF calculations show that the motion of the nuclei in the approach phase is close to that of rigid spheres [8], with the overlap region of the spheres defining the neck size. The neck only exceeds the geometric overlap slightly at the closest approach point. The geometric overlap assumption was used in refs. [2] and [3]. We shall improve the para-

meterization by assuming that the nuclear surfaces are sections of spheres with centers separated by the distance r, joined by a cylinder of such a radius to make a constant volume solid. The neck radius is obtained from the equation,

$$r_N^2(r - 2r_x) = [r_N^2 + \tfrac{1}{3}(R - r_x)^2](R - r_x)\,, \qquad (9)$$

where $r_x = (R^2 - r_N^2)^{1/2}$.

We emphasize that this parameterization is strictly for convenience in finding the r_n of TDHF: we do not imply that the system evolves with a constant volume or that it has a particular shape.

The neck evolution in the rebound phase is quite different. The neck shrinks rather slowly as the nuclei separate; the TDHF calculation of Dhar and Nilsson [8] obtains a neck shrinkage rate of 1/3 of the separation rate. To establish a function for the neck size in the rebounding phase, we assume a shape of two half spheres connected by two conical surfaces. The radius at the junction of the two cones is determined by fixing the volume of the system. The equation for r_n in the rebound phase is

$$r_n = \{[r^2R^2 - 4r(rR^2 - 4R^3)]^{1/2} - Rr\}/2r\,.$$

Despite the crudeness of these geometric assumptions, the model fits the neck evolution of the TDHF calculation of Dhar and Nilsson quite well, as may be seen from fig. 1.

The separation into two nuclei at the end of the rebound phase can take place by two different mechanisms. If the neck is too narrow in relation to its length, an instability driven by surface tension will cause the neck to pinch off. However, fast hydrodynamic flow is possible only when the single-particle wave functions are nodeless, requiring a small neck radius. We assume scission to occur when $r_n < 1$ fm. There is another mechanism for neck breakage when the nuclei rebound at high velocity. An instability develops with respect to density fluctuations when the bulk density falls below a critical value. According to ref. [9] this happens in mean field theory when the separation velocity exceeds $0.06c$. We shall assume that the neck snaps when the velocity is exceeded.

So far we have only considered the forces acting after the nuelei touch. Before they touch, the dynamics is well described by potential models, such as the proximity potential [10] or the Bass potential [11]. We shall use the Bass potential to describe the interaction before the nuclei touch. Particle exchange will also be included, using the parameterization of ref. [12].

We shall first examine the detailed motion in the collision $^{40}Ca + {}^{40}Ca$, to see how well our reduction to force dynamics works. We compare with TDHF

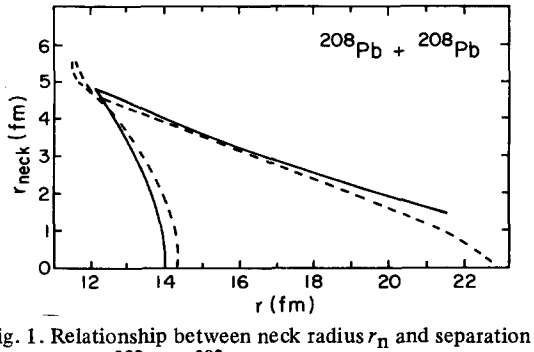

Fig. 1. Relationship between neck radius r_n and separation distance r for $^{208}Pb + {}^{208}Pb$ collisions at 800 MeV cm energy and zero impact parameter. The solid line is the present model, and the dashed line is from ref. [8].

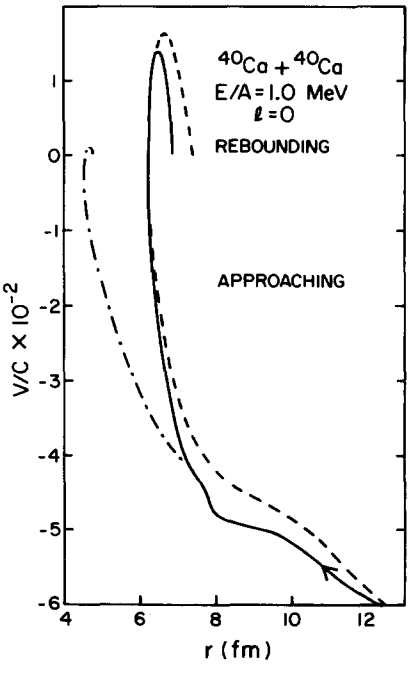

Fig. 2. History of $^{40}Ca + {}^{40}Ca$ collision at 80 MeV cm energy and zero impact parameter. The solid line shows the velocity as a function of separation distance, and the dashed line is a TDHF calculation by Weiss [13]. The dashed-dotted line shows the result of the force model in which the particle momentum flux is treated as a linear friction.

calculations by Weiss [13] in which r is evaluated as a function of time. In fig. 2 we plot dr/dt as a function of r, for a collision under conditions giving fusion. The figure shows the nuclei slowing down as they approach. At $r = 10$ fm the nuclear attraction is felt and the rate of slowing down diminishes. However, at $r = 6.5$ fm there is a sudden reversal of velocity, as if the nucleus had hit a hard wall and bounced elastically. The strong repulsive force at that point is due to the particle exchange. Our model reproduces that behavior with a memory time constant $\alpha = 1.8$ as shown by the dashed line. Under the assumption of extreme dissipation, $\alpha \sim 0$, and the repulsion does not last long enough to keep the nuclei from approaching to essentially form a spherical compound nucleus. That is shown as the dashed-dotted line in the figure.

We next examine the boundaries of the fusion regime for light nuclei. The TDHF fusion regime for $^{28}Si + ^{28}Si$ collisions [14] is shown in fig. 3, compared with our model. The low energy edge is determined by the potential field dynamics. An energy sufficient to surmount the potential barrier will cause the nuclei to touch, and they will remain fused due to the surface tension of the neck. At high impact parameter and energy the nuclei may scission after touching. The boundary line is determined essentially by the balance of centrifugal and surface forces, and may be described by a critical angular momentum. Finally,

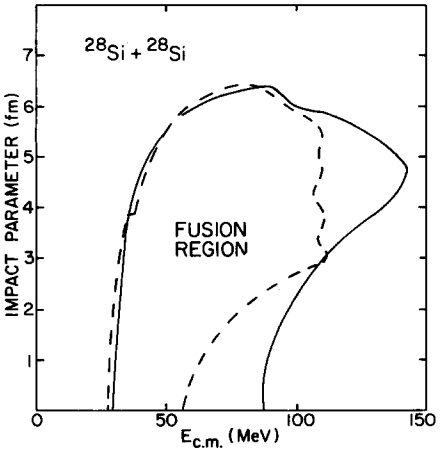

Fig. 3. Behavior of $^{28}Si + ^{28}Si$ collisions as a function of impact parameter and initial cm energy. The outer boundary shows the fusion region of the force model. The TDHF fusion prediction [14] is shown enclosed in the dashed line.

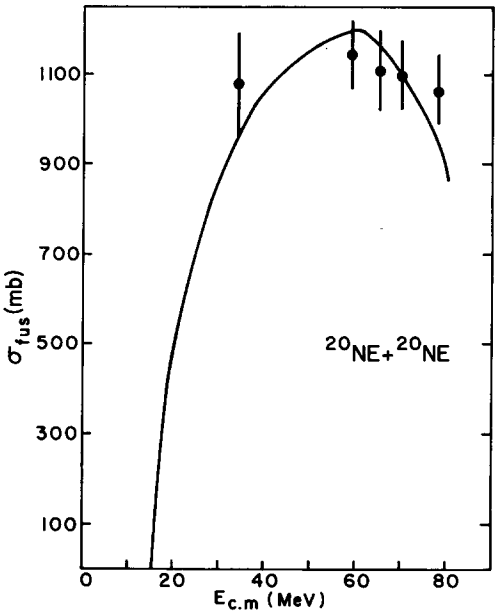

Fig. 4. The experimental fusion cross section for $^{20}Ne + ^{20}Ne$ collisions compared with the force model. The decrease in the predicted cross section at the highest energy is due to the opening of the fusion window.

there is a fusion window predicted in TDHF, which arises in our model because of the hard bounce behavior and the possibility of neck breakage at high rebound velocities. Other force models do not have this characteristic feature of TDHF. The comparison of TDHF with our model in fig. 3 shows that all the qualitative features of TDHF can be described with force dynamics.

However, actual nuclear collisions probably do not exhibit fusion windows. In fig. 4 we show the measured fusion cross section [15] for $^{20}Ne + ^{20}Ne$ compared with the force model. The experimental cross section is rather constant, even at energies where the fusion window should be evident. Evidently, TDHF is inadequate at the higher energies. Nucleon–nucleon collisions will become important and may affect the force dynamics in several ways. For example, the memory time will be shorter if the system is thermalized by n–n collisions. This will reduce the magnitude of the bounce, leading to more sticking behavior.

We acknowledge the support of the National Science Foundation, and the support of "Fondazione Angelo Della Riccia" for A. Bonasera.

References

[1] G. Bertsch, MSU preprint (1982).
[2] D. Gross and H. Kalinowski, Phys. Rep. 45 (1978) 175.
[3] F. Beck et al., Phys. Lett. 76B (1978) 35.
[4] D.M. Brink and Fl. Stancu, Phys. Rev. C24 (1981) 144.
[5] A. Abrikosov and I. Khalatnikov, Rep. Prog. Phys. 22 (1959) 336, eq. (6.3).
[6] J. Randrup, Ann. Phys. (NY) 112 (1978) 356.
[7] A. Jain and N. Sarma, Phys. Rev. C24 (1981) 1066.
[8] A. Dhar and B. Nilsson, Phys. Lett. 77B (1978) 50.
[9] G. Bertsch and D. Mundinger, Phys. Rev. C17 (1978) 1646.
[10] J. Blocki et al., Ann. Phys. (NY) 105 (1977) 427.
[11] R. Bass, Phys. Rev. Lett. 39 (1977) 265.
[12] C.M. Ko et al., Phys. Lett. 77B (1978) 174.
[13] M. Weiss, private communication.
[14] P. Bonche et al., Phys. Rev. C20 (1979) 641.
[15] D. Shapiro et al., Phys. Rev. C28 (1983) 1148.